IEEE Access
Multidisciplinary | Rapid Review | Open Access Journal

Received June 4, 2020, accepted June 16, 2020, date of publication June 18, 2020, date of current version June 30, 2020.

Digital Object Identifier 10.1109/ACCESS.2020.3003530

Statistical Analysis of Antenna Efficiency Measurements With Non-Reference Antenna Methods in a Reverberation Chamber

WEI XUE[1], (Student Member, IEEE), XIAOMING CHEN[1], (Senior Member, IEEE), MING ZHANG[1], (Member, IEEE), LUYU ZHAO[2], (Senior Member, IEEE), ANXUE ZHANG[1], (Member, IEEE), AND YI HUANG[3], (Senior Member, IEEE)

[1]School of Information and Communications Engineering, Xi'an Jiaotong University, Xi'an 710049, China
[2]Key Laboratory of Antennas and Microwave Technologies, Xidian University, Xi'an 710071, China
[3]Department of Electrical Engineering and Electronics, University of Liverpool, Liverpool L69 3GJ, U.K.

Corresponding author: Xiaoming Chen (xiaoming.chen@mail.xjtu.edu.cn)

This work was supported in part by the National Natural Science Foundation of China under Grant 61801366, in part by the Natural Science Foundation of Shaanxi Province under Grant 2020JM-078, and in part by the Innovation Team Research Fund of Shaanxi Province under Grant 2019TD-013.

ABSTRACT Reverberation chambers (RCs) have become a popular testing facility in antenna efficiency measurements. Unlike the standard reference antenna method, the non-reference antenna methods have been proposed to measure the antenna efficiency in the absence of a reference antenna. However, the statistical distributions of the measured (estimated) total antenna efficiencies using the non-reference antenna methods have not been derived before, making it difficult to perform a rigorous statistical analysis of the antenna efficiency measurement. In this paper, the distributions of the measured total antenna efficiencies using two non-reference antenna methods in an RC are derived, based on which the statistics (e.g., expectation and variance) of the measured total antenna efficiencies are also derived. It is shown that the original non-reference antenna methods (estimators) are only asymptotically unbiased and are biased with limited samples, thus corresponding unbiased estimators are proposed and analyzed. The derived analytical expressions of the statistics of the total antenna efficiency estimators are verified by simulations and measurements in an RC. The performances of different non-reference antenna methods are discussed.

INDEX TERMS Antenna efficiency, measurement uncertainty, non-reference antenna methods, reverberation chamber.

I. INTRODUCTION

The reverberation chamber (RC) is an electrically large conducting cavity equipped with metallic mode stirrers, which can stir the electromagnetic modes through mechanical rotations [1], [2]. Due to complicated boundary conditions, electromagnetic modeling of the RC can be computationally expensive, e.g., [3]. Hence, the field in the RC is usually modeled as stochastic process. Specifically, the field inside a well-stirred RC is considered to be random and statistically homogeneous. The RC is traditionally used for electromagnetic compatibility (EMC) tests and measurements [1], [4]. Due to its particular properties (e.g., low cost, high efficiency, and good repeatability), the RC has been applied to various over-the-air tests [5]–[7]. Unlike the multi-probe anechoic chamber method [8], the RC is extremely suitable for large-form-factor single-antenna equipment [9]. One of the important applications is antenna measurements to determine the antenna characteristics. In the past few years, many RC-based methods have been proposed for accurate and efficient measurements to determine antenna characteristics, such as antenna efficiency (using the standard reference antenna method [4], the emission-based method [10], the non-reference antenna methods [11], the time-domain method [12], [13], the nested and contiguous RCs method [14], the open-ended waveguide-plate method [15], the quality factor method [16], etc.), free-space S-parameter [17], [18], radiation pattern (using the

The associate editor coordinating the review of this manuscript and approving it for publication was Giorgio Montisci.

plane wave decomposition method [19], the intensity-based method [20], the K-factor method [21], the time-reversal method [22], the spherical wave decomposition method [23], etc.), and diversity gain and capacity of multiple-input multiple-output (MIMO) antennas [24], [25]. In this work, however, we focus on the measurement of the antenna efficiency.

Most of the methods for antenna efficiency measurements dictate a reference antenna. The standard reference antenna method [4] is perhaps the most popular one. The statistics of the measured total antenna efficiency using the standard reference antenna method have been studied in [26], which allows more insight to the uncertainty of the standard reference antenna method. Yet, this method requires a reference antenna with known efficiency, which may not be available for the desired working frequency band in practice. In order to solve the problem, non-reference antenna methods, i.e., one-, two-, and three-antenna methods, were proposed in [11]. These methods are derived based on the quality factors (Q) in time and frequency domains and eliminate the need of a reference antenna. Since different non-reference antenna methods have different prerequisites and measurement setups, these methods possess different measurement uncertainties. It should be noted that the measurement uncertainties have been analyzed semi-empirically in [11]. Nevertheless, the semi-empirical analyses mainly focus on the measurement uncertainties of the entire measurement system, which are caused by the measurements of S-parameters, the fluctuation of measurement facilities, and the inconsistence of the measurement environment, whereas the statistical distribution of the measured (estimated) total antenna efficiency is still unknown to date.

In previous work [26], the statistics of the reference antenna method has been derived. However, the statistical distributions of the measured total antenna efficiencies using the three non-reference antenna methods [11] are still unknown to date. In this work, we have derived the distributions and associated statistics of two non-reference antenna methods (i.e., the one-antenna method and the three antenna method), based on which rigorous statistical analyses of the uncertainties of the methods are performed. Specifically, the probability density functions (PDF) and related statistics [e.g., expectation, variance, and mean square error (MSE)] are derived. Both simulations and measurements are performed to verify the derived PDFs and statistics. Good agreements are observed. The distribution of the two-antenna method is still unknown to date.

The rest of this paper is organized as follows: Section II briefly introduces the three non-reference antenna methods, and presents detailed derivations of the PDFs and related statistics. Numerical simulations and RC measurements are performed to verify the derived PDFs and associated statistics in Sections III and IV, respectively. Finally, Section V concludes this paper.

II. STATISTICS OF MEASURED ANTENNA EFFICIENCY

For the sake of completeness and to facilitate the deviation of the distributions, three non-reference antenna methods are briefly introduced below.

A. ONE- AND TWO-ANTENNA METHODS

A common setup for antenna efficiency measurements using the one-antenna method is shown in Fig. 1. The vector network analyzer (VNA) and the motor controller are connected to a computer, which controls the rotation of stirrers and the collection and storage of the measured S-parameters. Assuming that Antenna 1 is connected to Port 1 of the VNA, the power accepted at the antenna port is denoted as P_t and the power radiated by the antenna is denoted as P_{TX}. Once the power is radiated into the chamber, it will be bounded back and forth in the RC by the chamber walls and the stirrers. A portion of the stirred power will be received by the antenna again (referred to as P_{RF} hereafter). The received power P_{RF} undergoes antenna mismatch and reduces to P_{rf} at the VNA port.

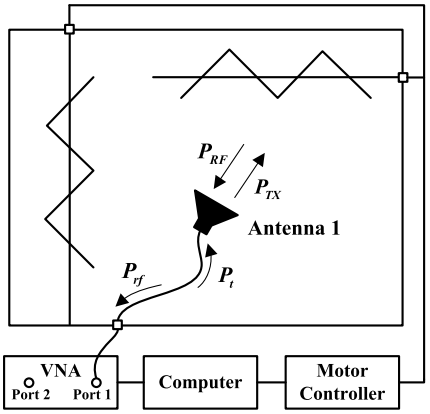

FIGURE 1. Measurement setup for the one-antenna method.

According to [11], once different samples of S_{11} at different stirring conditions are measured by the VNA, the antenna efficiency of Antenna 1 can be calculated as

$$\hat{e}_1 = \sqrt{\frac{C_{RC}}{2Q}\langle |S_{11,m,s}|^2 \rangle}, \tag{1}$$

where $C_{RC} = 16\pi^2 V/\lambda^3$ with V being the volume of the RC and λ being the wavelength, $|S_{11,m}|^2 = P_{rf}/P_t$ includes the effect of imperfect antenna efficiency (i.e., $e_1 < 1$), and $S_{11,m,s} = S_{11,m} - \langle S_{11,m} \rangle$ represents the stirred part of the $S_{11,m}$ with $\langle \cdot \rangle$ denoting the ensemble average. Q is the quality factor of the RC and obtained using the time-domain method, i.e., $Q = w\tau_{\mathrm{RC}}$(where τ_{RC} is the chamber decay time). The time-domain Q is only associated with the chamber losses (not associated with the antenna losses) [1], [11], [27]. It should be stressed that Q is considered as a constant for the convenience of analyses in this work. In this paper, e_1 denotes

the true antenna efficiency of the antenna under test, while $\hat{e}_1$ is the estimate of e_1 from measurements. Obviously, e_1 is a constant for a specified antenna under test at a given frequency. $\hat{e}_1$, on the other hand, is a random variable that follows certain distribution (as discussed later).

It should be noted that the one-antenna method has a prerequisite that the enhanced backscatter coefficient (e_b) is equal to two [1], [28], that is

$$e_{b1} = \frac{\langle |S_{11,s}|^2 \rangle}{\langle |S_{21,s}|^2 \rangle} = 2. \tag{2}$$

It is obvious that

$$\begin{aligned} P_{TX} &= e_1 P_t \\ P_{rf} &= e_1 P_{RF}. \end{aligned} \tag{3}$$

Thus (1) can be rewritten as

$$\hat{e}_1 = e_1 \sqrt{\frac{C_{RC}}{2Q} \langle |S_{11,,s}|^2 \rangle}, \tag{4}$$

where $|S_{11}|^2 = P_{RF}/P_{TX}$ represents the ideal return loss excluding the effect of the antenna efficiency. Note that (4) indicates the relationship between the estimator of the antenna efficiency and the true antenna efficiency.

In a well-stirred RC, $X = |S_{21,s}|^2$ follows the exponential distribution [1]

$$f(x) = \frac{C_{RC}}{Q} \exp\left(-\frac{C_{RC}}{Q} x\right). \tag{5}$$

One can conclude from (2) and (5) that $Y = |S_{11,s}|^2 = 2|S_{21,s}|^2$ also follows the exponential distribution

$$f(y) = \frac{C_{RC}}{2Q} \exp\left(-\frac{C_{RC}}{2Q} y\right). \tag{6}$$

For independent and identically distributed (IID) Y_i ($i = 1, 2, \ldots, N$) that follows the exponential distribution, $U = \sum_N Y_i = \sum_N |S_{11,s}|^2$ follows the gamma distribution [29]

$$f(u) = \frac{B^N}{\Gamma(N)} u^{N-1} \exp(-Bu), \tag{7}$$

where $B = C_{RC}/2Q$ and Γ is the Gamma function [30]. If N is an integer, $\Gamma(N) = (N-1)!$, where ! is the factorial operator.

Since C_{RC}, Q, N are constants, the PDF of $T = \sqrt{BU/N}$ can be derived based on (7) as,

$$f(t) = \frac{2N^N}{\Gamma(N)} t^{2N-1} \exp(-Nt^2). \tag{8}$$

For notational convenience, we denote $\hat{e}_1 = e_1 T$ as $G = e_1 T$, whose PDF can be easily derived as

$$f(g; e_1) = \frac{2N^N}{\Gamma(N) e_1^{2N}} g^{2N-1} \exp(-\frac{Ng^2}{e_1^2}). \tag{9}$$

Once we obtain the PDF of $\hat{e}_1$ (i.e., G), the statistics of $\hat{e}_1$ can be readily derived. The expectation and variance of $\hat{e}_1$ are given as

$$\begin{aligned} E(\hat{e}_1) &= \frac{\Gamma(2N+1)}{\Gamma(N+1)^2} \frac{\sqrt{\pi N}}{2^{2N}} e_1 \\ VAR(\hat{e}_1) &= \left\{ 1 - \frac{\pi N}{2^{4N}} \frac{\Gamma(2N+1)^2}{\Gamma(N+1)^4} \right\} e_1^2, \end{aligned} \tag{10}$$

where E and VAR denote the expectation and variance operators, respectively. (Please refer to Appendix A for their derivations.)

According to the jargons of statistics and estimation theory, the bias of an estimator is the discrepancy between the expectation of the estimator and the true value of the parameter being estimated. An estimator without any bias is referred to as unbiased estimator, otherwise it is biased. It can be seen from (10) that the efficiency estimator (1) is asymptotically unbiased, i.e., the expectation approaches e_1 and the variance approaches zero as N approaches infinity. Nevertheless, (1) is a biased estimator with limited samples. Based on (10), an unbiased estimator ($\hat{e}_1^{unbiased}$) can be proposed by aiming $E(\hat{e}_1^{unbiased}) = e_1$

$$\hat{e}_1^{unbiased} = \frac{\Gamma(N+1)^2}{\Gamma(2N+1)} \frac{2^{2N}}{\sqrt{\pi N}} \sqrt{\frac{C_{RC}}{2Q} \langle |S_{11,m,s}|^2 \rangle}. \tag{11}$$

The expectation and variance of the unbiased estimator (11) can be derived as

$$\begin{aligned} E\left(\hat{e}_1^{unbiased}\right) &= e_1 \\ VAR\left(\hat{e}_1^{unbiased}\right) &= \left\{ \frac{2^{4N}}{\pi N} \frac{\Gamma(N+1)^4}{\Gamma(2N+1)^2} - 1 \right\} e_1^2. \end{aligned} \tag{12}$$

The root mean square (RMS) of $\hat{e}_1$ and $\hat{e}_1^{unbiased}$ can be readily derived based on (10) and (12) as

$$RMS(\hat{e}_1) = e_1. \tag{13}$$

$$RMS(\hat{e}_1^{unbiased}) = e_1 \frac{2^{2N} \Gamma(N+1)^2}{\Gamma(2N+1)} \frac{1}{\sqrt{\pi N}}. \tag{14}$$

Note that $RMS(X) = \sqrt{E(X^2)} = \sqrt{VAR(X) + [E(X)]^2}$, given (10), the RMS of $\hat{e}_1$ boils down to the true value e_1.

Since (1) is a biased estimator, the MSE

$$MSE(\hat{e}_1) = E\left[(\hat{e}_1 - e_1)^2\right] = \left[2 - \frac{\Gamma(2N+1)}{\Gamma(N+1)^2} \frac{\sqrt{\pi N}}{2^{2N-1}} \right] e_1^2, \tag{15}$$

is a more appropriate metric to evaluate its performance. It is noted that for the unbiased estimator, the MSE is equal to its variance.

The Cramer - Rao lower bound (CRLB) offers a lower bound on the variance of the unbiased estimator (i.e., $VAR(\hat{e}^{unbiased}) \geq CRLB(e)$ holds for any unbiased estimator $\hat{e}^{unbiased}$) [31], [32]. The unbiased estimator performs better if its variance is closer to the CRLB. Thus the CRLB is an important metric to evaluate the performance of the unbiased

estimator. The CRLB of the unbiased estimator (11) is derived in Appendix A.

The two-antenna method can be derived based on the one-antenna method. The measurement setup is similar to Fig. 1, the only difference is that another antenna (i.e., Antenna 2) is connected to Port 2 of the VNA. (For the sake of conciseness of the paper, the graphic illustration of the measurement setup of the two-antenna method is omitted here.) The antenna efficiencies of the two antennas can be calculated as [11]

$$\hat{e}_i = \sqrt{\frac{C_{RC}}{Q}\frac{\langle|S_{ii,m,s}|^2\rangle}{e_b}}, \tag{16}$$

where $e_b = \sqrt{\langle|S_{11,m,s}|^2\rangle\langle|S_{22,m,s}|^2\rangle}\Big/\langle|S_{21,m,s}|^2\rangle$ and $\hat{e}_i$ represents the estimate of the efficiency of Antenna i $(i = 1, 2)$.

The two-antenna method is similar to the one-antenna method, except that the prerequisite of e_b is relaxed to some extent [11]. If we simply suppose the enhanced backscatter coefficient equals two, the statistics of the two-antenna method will be the same as that of the one-antenna method. However, if e_b is calculated using $e_b = \sqrt{\langle|S_{11,m,s}|^2\rangle\langle|S_{22,m,s}|^2\rangle}\Big/\langle|S_{21,m,s}|^2\rangle$ strictly, the distribution is still unknown to date. We only present the derived statistics of the one-antenna method here.

B. THREE-ANTENNA METHOD

A common setup for antenna efficiency measurements using the three-antenna method is shown in Fig. 2. There are three antennas in the RC, i.e., Antenna 1, Antenna 2, and Antenna 3. In order to measure the antenna efficiencies with a two-ports VNA, measurements are conducted between every two antennas. The antennas not connected to the VNA are terminated with a 50 ohm load.

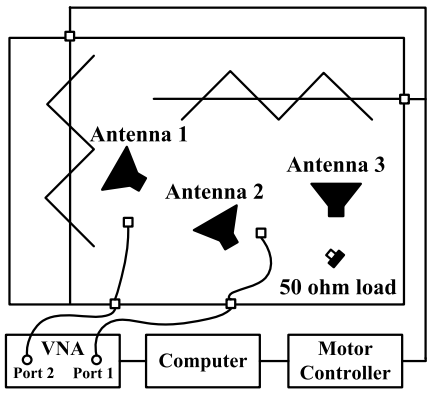

FIGURE 2. Measurement setup for the three-antenna method. The antennas not connected to the VNA are connected on a 50 ohm load.

Once all the measurements are completed, the antenna efficiencies can be obtained as [11]

$$\begin{aligned}
\hat{e}_1 &= \sqrt{\frac{C_{RC}}{Q}\frac{\langle|S_{21,m,s}|^2\rangle\langle|S_{31,m,s}|^2\rangle}{\langle|S_{32,m,s}|^2\rangle}} \\
\hat{e}_2 &= \sqrt{\frac{C_{RC}}{Q}\frac{\langle|S_{21,m,s}|^2\rangle\langle|S_{32,m,s}|^2\rangle}{\langle|S_{31,m,s}|^2\rangle}} \\
\hat{e}_3 &= \sqrt{\frac{C_{RC}}{Q}\frac{\langle|S_{31,m,s}|^2\rangle\langle|S_{32,m,s}|^2\rangle}{\langle|S_{21,m,s}|^2\rangle}}.
\end{aligned} \tag{17}$$

Since the efficiency estimates of the three antennas have the same form, the corresponding PDFs should also have the same form. For the sake of conciseness, we take the efficiency of Antenna 1 for instance to derive the statistics of the three-antenna method. Following the same thought of excluding the effect of the antenna efficiency from $S_{11,m}$, the efficiency estimate of Antenna 1 in (17) can be rewritten as

$$\hat{e}_1 = e_1\sqrt{\frac{C_{RC}}{Q}\frac{\langle|S_{21,s}|^2\rangle\langle|S_{31,s}|^2\rangle}{\langle|S_{32,s}|^2\rangle}}. \tag{18}$$

As discussed in the previous subsection, $X = |S_{21,s}|^2$ follows the exponential distribution. Since $|S_{21,s}|^2$, $|S_{31,s}|^2$, and $|S_{32,s}|^2$ are measured in the same RC, they all have the same PDF. Based on (5), we can derive the PDF of $Z = \sqrt{\langle|S_{21,s}|^2\rangle\langle|S_{31,s}|^2\rangle}$ as [33]

$$f(z) = \frac{4NA^{2N}}{\Gamma(N)^2}(Nz)^{2N-1}K_0(2NAz), \tag{19}$$

where $A = C_{RC}/Q$, $K_0(x)$ is the zero-order modified Bessel function of the second kind [30].

In order to derive the PDF of (18), we denote $\hat{e}_1 = e_1 W = e_1 Z/V$, where $V = \sqrt{\langle|S_{32,s}|^2\rangle}/A$. The PDF of V can be derived based on (5) as

$$f(v) = \frac{2N^N A^{2N}}{\Gamma(N)}v^{2N-1}e^{-A^2Nv^2}. \tag{20}$$

Combining (19) and (21), the PDF of W can be derived as

$$\begin{aligned}
f(w) &= \int f_Z(wv)f_V(v)\,|v|\,dv \\
&= \frac{2\Gamma(2N)^2}{\Gamma(N)^3N^Nw^{2N+1}}{}_2F_0(2N, 2N; ; -\frac{1}{Nw^2}),
\end{aligned} \tag{21}$$

where ${}_pF_q(a_1, \ldots, a_p; b_1, \ldots, b_q; x)$ is the generalized hypergeometric function that possesses p parameters of type 1 and q parameters of type 2 [30].

Similar to the one-antenna method, we denote $\hat{e}_1 = e_1 W$ as $R = e_1 W$, whose PDF can be easily derived as

$$f(r; e_1) = \frac{2\Gamma(2N)^2e_1^{2N}}{\Gamma(N)^3N^Nr^{2N+1}}{}_2F_0(2N, 2N; ; -\frac{e_1^2}{Nr^2}). \tag{22}$$

(Please refer to Appendix B for its derivation.)

Once we obtain the PDF of $\hat{e}_1$ (i.e., R), the statistics of $\hat{e}_1$ can be readily derived. The expectation and variance of $\hat{e}_1$ can be derived from (22) as

$$E\left(\hat{e}_1\right) = \frac{\Gamma(N+\frac{1}{2})^2\Gamma(N-\frac{1}{2})}{\sqrt{N}\Gamma(N)^3}e_1$$
$$VAR\left(\hat{e}_1\right) = \left[\frac{\Gamma(N+1)^2\Gamma(N-1)}{N\Gamma(N)^3} - \frac{\Gamma(N+\frac{1}{2})^4\Gamma(N-\frac{1}{2})^2}{N\Gamma(N)^6}\right]e_1^2. \tag{23}$$

(Please refer to Appendix B for their derivations.)

It can be seen from (23) that the efficiency estimator (17) is also asymptotically unbiased and biased with limited samples. Therefore, an unbiased estimator is proposed based on (23)

$$e_1^{unbiased} = \frac{\sqrt{N}\Gamma(N)^3}{\Gamma(N+\frac{1}{2})^2\Gamma(N-\frac{1}{2})} \times \sqrt{\frac{C_{RC}}{Q}\frac{\langle|S_{21,m,s}|^2\rangle\langle|S_{31,m,s}|^2\rangle}{\langle|S_{32,m,s}|^2\rangle}}. \tag{24}$$

The expectation and variance of the unbiased estimator (24) are

$$E\left(\hat{e}_1^{unbiased}\right) = e_1$$
$$VAR\left(\hat{e}_1^{unbiased}\right) = \left[\frac{\Gamma(N)^3\Gamma(N+1)^2\Gamma(N-1)}{\Gamma(N+\frac{1}{2})^4\Gamma(N-\frac{1}{2})^2} - 1\right]e_1^2. \tag{25}$$

The corresponding RMS can be derived from (23) and (25) as

$$RMS(\hat{e}_1) = e_1\frac{\Gamma(N+1)}{\Gamma(N)}\sqrt{\frac{\Gamma(N-1)}{N\Gamma(N)}}. \tag{26}$$
$$RMS(\hat{e}_1^{unbiased}) = e_1\frac{\Gamma(N)\Gamma(N+1)}{\Gamma(N+\frac{1}{2})^2\Gamma(N-\frac{1}{2})}\sqrt{\Gamma(N)\Gamma(N-1)}. \tag{27}$$

The MSE can be derived from (23) as

$$MSE\left(\hat{e}_1\right) = \left[\frac{\Gamma(N+1)^2\Gamma(N-1)}{N\Gamma(N)^3} - \frac{2\Gamma(N+\frac{1}{2})^2\Gamma(N-\frac{1}{2})}{\sqrt{N}\Gamma(N)^3} + 1\right]e_1^2. \tag{28}$$

The MSE of the unbiased estimator (24) equals its variance (25). The CRLB of the unbiased estimator (24) is derived in Appendix B. As mentioned before, the estimates of Antenna 2 and Antenna 3 possess the same PDF and statistics as Antenna 1 and, therefore, are omitted here for the sake of conciseness.

III. SIMULATIONS

In this section, Monte Carlo simulations are conducted to verify the derived PDFs and associated statistics of the non-reference antenna methods. For each number of independent samples N, we randomly generate $1000 \times N$ IID samples

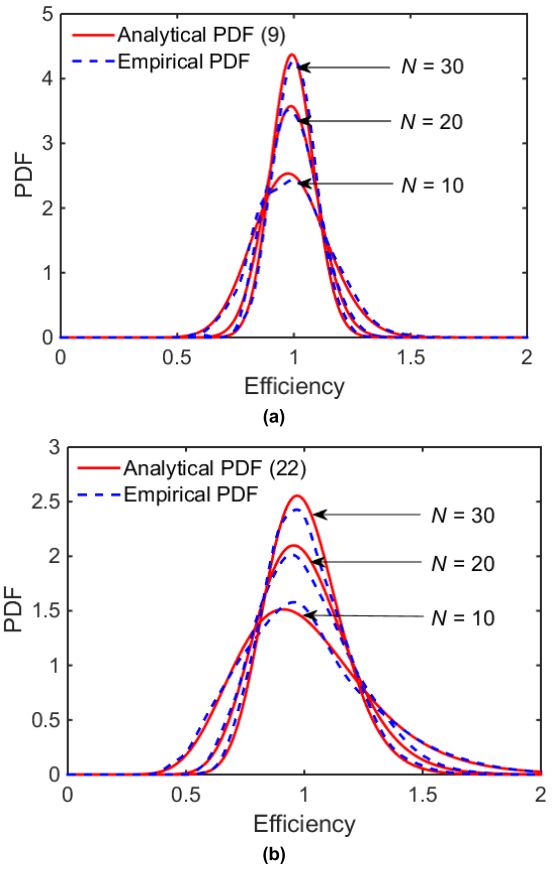

FIGURE 3. Comparisons of the empirical and analytical PDFs of (a) one-antenna method and (b) three-antenna method with different values of N when $e_1 = 1$.

that follow the exponential distribution, i.e., $1000 \times N$ realizations of $Y = |S_{11,s}|^2 \sim Exp(C_{RC}/2Q)$ for the one-antenna method and $1000 \times N$ realizations of $X = |S_{21,s}|^2$, $|S_{31,s}|^2$, and $|S_{32,s}|^2 \sim Exp(C_{RC}/Q)$ for the three-antenna method. Thus we have 1000 realizations of $\hat{e}_1$ for each case of N and for both methods. The empirical PDF, expectation, variance, and other statistics can be readily obtained.

Fig. 3 shows that the empirical PDFs and the corresponding analytical PDFs for the two non-reference antenna methods [i.e., (9) and (22)] with different values of N when $e_1 = 1$. It can be seen that the analytical PDFs agree well with their empirical counterparts, which proves the correctness of the derived PDFs. Furthermore, it can be observed that, as N increases, the shapes of PDFs (9) and (22) become sharper and the distributions concentrate on the true antenna efficiency (i.e., 100%).

As shown in Fig. 3, the measured antenna efficiency has certain probability (e.g., about 50% for the one- and the three-antenna method when $N = 30$) of being no smaller than the true antenna efficiency (i.e., 100%), which results in the invalid measurement results in practice. Moreover, there will always be a nonzero probability (small as it may be) that the measured antenna efficiency (in an RC) is larger

than 100%, even we gather hundreds of samples (much more than 30) to determine the antenna efficiency. For a simple antenna efficiency measurement, the invalid results should be discarded. However, if we discard all the measured results that above or equal to 100%, the estimated expectation value will be lower than the true value (i.e., 100%). Hence, whether the measured results should be discarded depends on the purpose of the measurements. For antenna efficiency measurements, we should of course discard those values that are larger than 100%. Nevertheless, for statistical analysis of the measurement uncertainty, we cannot omit those values because we need them to verify the derived PDF and related statistics.

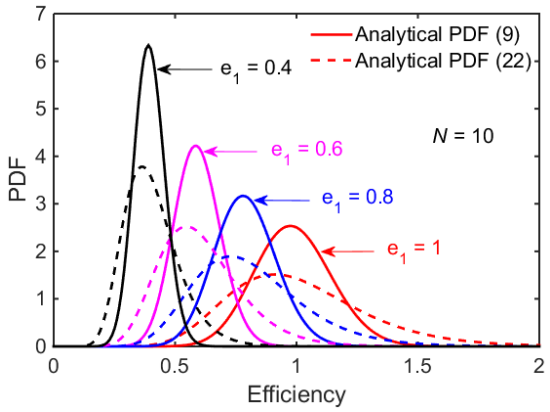

FIGURE 4. Comparison of the analytical PDFs of the one- and three-antenna methods for different values of e_1 when $N = 10$.

Note that the PDFs are function of e_1. Fig. 4 shows the analytical PDFs of the two non-reference antenna methods for different values of e_1 when $N = 10$. It can be seen that the shapes of the PDFs become sharper as e_1 decreases. In other words, the measurement uncertainty is smaller for an antenna with lower efficiency. This is also reflected by the fact that the variance and MSE of $\hat{e}_1$ is proportional to the square of e_1 (cf. Section II). Hence, the absolute error becomes smaller as the true antenna efficiency decreases. This should not come as a surprise. Because, given a fixed relative error, the lower the true value is, the lower the absolute error will be. To be exact, the absolute error is related to the efficiency of the antenna under test, while the relative error is not. Combining Figs. 3 and 4, we can conclude that PDF (9) is sharper than PDF (22) for the same N and e_1.

To facilitate the analysis and comparison of the simulation results and without loss of generality, the antenna efficiency is assumed to be unity (i.e., $e_1 = 1$) hereafter in this section. Fig. 5 shows the empirical and analytical expectations and variances, and analytical RMSs and MSEs of estimators (1) and (11) of the one-antenna method. It can be seen that the empirical expectation and variance are in accordance with the analytical ones, verifying the correctness of the derived expressions of the analytical expectation and variance. Since the RMS and MSE can be expressed using the

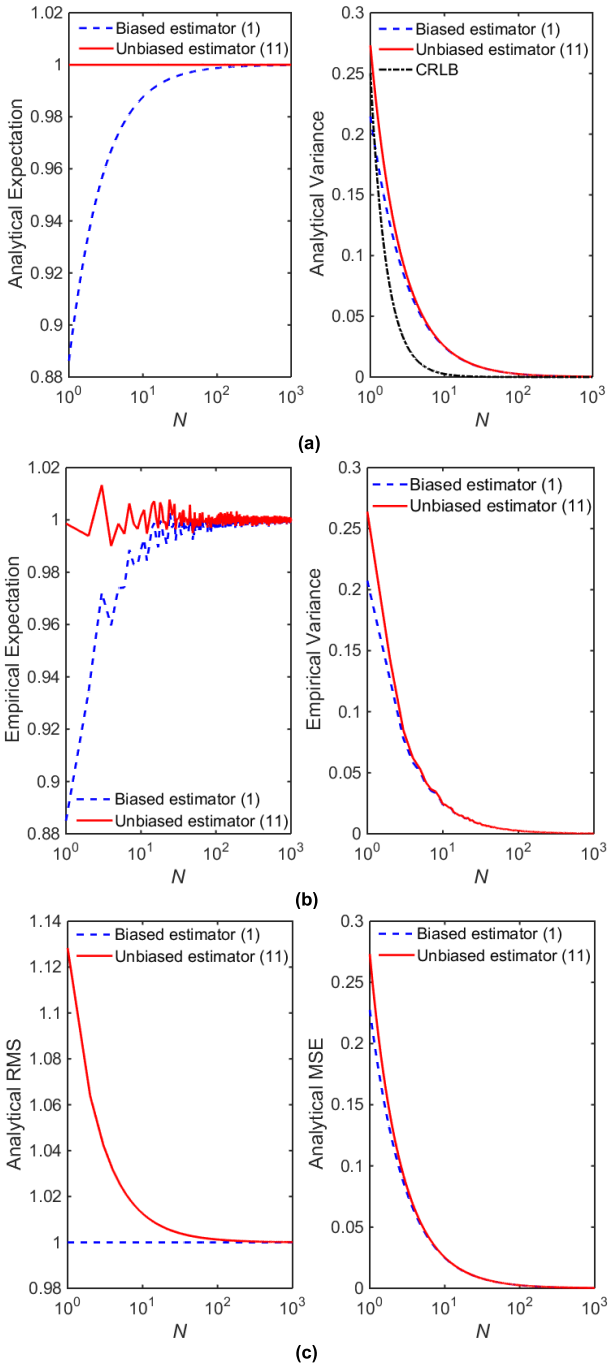

FIGURE 5. Statistics of the one-antenna method: (a) analytical expectation, variance (together with CRLB), (b) empirical expectation and variance, and (c) analytical RMS and MSE.

expectation and variance, it is self-evident that the analytical RMS and MSE are also correct. For the sake of conciseness, the empirical RMS and MSE are omitted here. It can be observed from Fig. 5 that, when N is small, the unbiased estimator (11) performs better in estimating the expectation but worse in estimating the variance, RMS, and MSE than the biased estimator (1). As N increases, the gap of the statistics between estimators (1) and (11) diminishes rapidly. For the

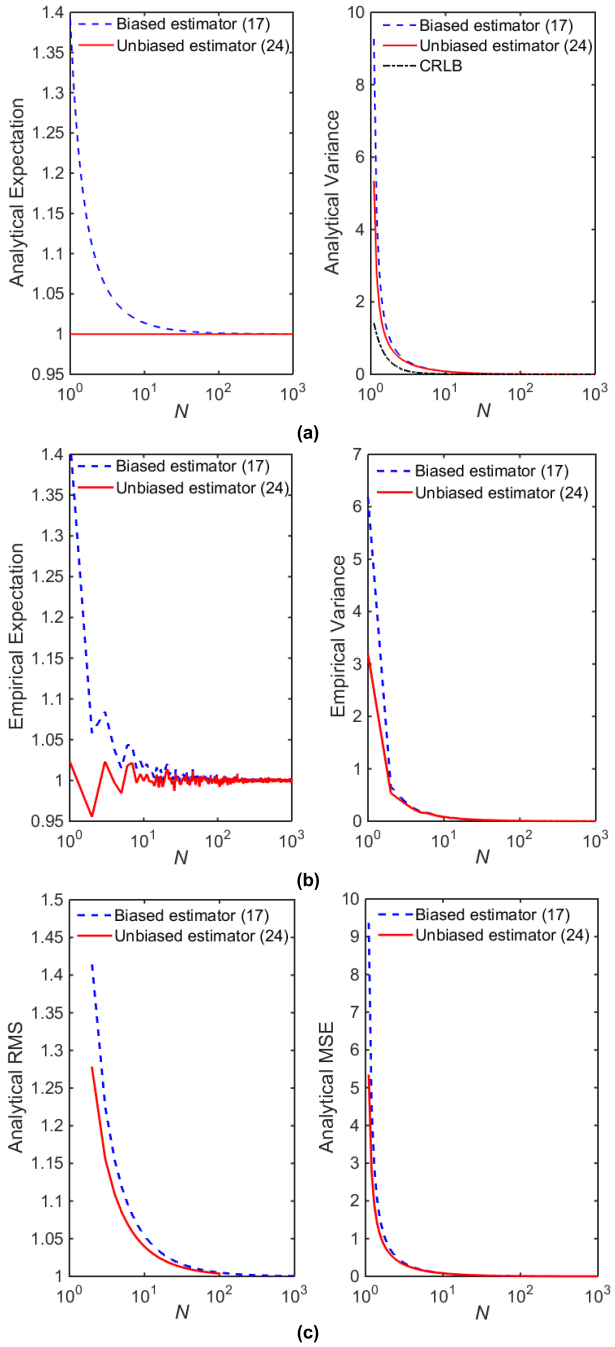

FIGURE 6. Statistics of the three-antenna method: (a) analytical expectation, variance (together with CRLB), (b) empirical expectation and variance, and (c) analytical RMS and MSE.

expectation and RMS, the differences between estimators (1) and (11) become indistinguishable for $N > 100$. For the variance and MSE, the differences between estimator (1) and (11) become indistinguishable for $N > 10$. Note that the CRLB is also plotted in Fig. 5(a). As can be seen, the variance of estimator (11) is above the CRLB as expected.

Fig. 6 shows the empirical and analytical expectations and variances, and analytical RMSs and MSEs of estimator (17) and (24) of the three-antenna method. In order to be consistent with the one-antenna method, the statistics are also plotted from $N = 1$ to 10^3, although some of the analytical statistics do not exist when $N = 1$. It can be seen that the empirical expectation and variance are in accordance with the analytical ones. Different with the one-antenna method, the unbiased estimator (24) outperforms the biased estimator (17) for small N. As N increases, the gap of the statistics between estimators (17) and (24) decreases rapidly. As expected, the variance of estimator (24) is above the CRLB. For the expectation and RMS, the difference between estimators (17) and (24) diminishes for $N > 100$. For the variance and MSE, the difference between estimators (17) and (24) diminishes for $N > 10$.

Comparing Figs. 5 and 6, it can be seen that the one-antenna method suffers from underestimation with limited samples, whereas the three-antenna method suffers from overestimation with limited samples. For both methods, the expectation, variance, RMS, and MSE convergence to the same value as N increases. Since the one-antenna method enjoys a faster convergence rate and results in a smaller bias than the three-antenna method does, it should perform slightly better than the three-antenna method.

IV. MEASUREMENTS

In order to verify the PDFs and statistics of the non-reference antenna methods further, extensive measurements are performed from 2.4 to 3.6 GHz in an RC. The RC has a size of 1.50 m × 1.44 m × 0.92 m with a lowest usable frequency of about 0.87 GHz [34]. As shown in Fig. 7, the RC contains two mechanical stirrers (one vertical and one horizontal) and a turn-table platform. A trestle with adjustable height and

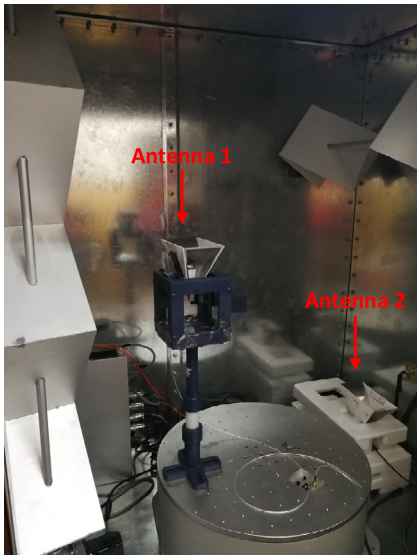

FIGURE 7. Setup for antenna efficiency measurement using the one-antenna method and three-antenna method. Antenna 3 is located behind the vertical mode stirrer in the left and, therefore, not shown in the photo. Antenna 1 has three orientations throughout the measurements. Only the vertical orientation is shown here.

orientation is used to support the antenna on the turn-table platform. Three double-ridged horn antennas (referred to Antennas 1, 2, and 3 hereafter) with slightly different sizes yet the same working frequency band are selected to conduct the measurements. The distance between the antennas under test and the nearest metallic object is more than one wavelength at the lowest testing frequency. In this way, we make sure the antennas under test are within the working volume of the RC, where the fields is (statistically) uniformly distributed. For reasons mentioned in Section II, we focus on the one- and three-antenna method in the measurements. To ensure that the RC has the same loading condition for the measurements using the two methods, all the antennas and supporters are placed in the RC during the whole measurement procedure, and the antennas not connected to the VNA are connected on a 50 ohm load.

During the measurements, the turn-table platform moves step-wise to 10 angles that are evenly distributed over one complete rotation. At each platform rotation angle, the two stirrers move simultaneously and step-wise to 10 angles that are evenly distributed over one complete rotation. The S-parameters are sampled and recorded by the VNA with a frequency step of 1 MHz at each stirrer position. Hence, for each measurement, we have 100 samples from mechanical stirring.

In order to characterize the statistics of the antenna efficiency estimators, the nine-case assessment procedure [35]–[37] is adopted in this work. That is the measurements using the two non-reference antenna methods are repeated for nine cases: the trestle is adjusted to three heights (i.e., 15, 30, 45 cm), and the antenna on the trestle is orientated in the vertical and two horizontal orientations (in radial and tangential directions of the platform) at each height. The distance between every two adjacent heights is larger than one wavelength at the lowest frequency (i.e., 2.4 GHz) and the three orientations are orthogonal, making sure that the nine-case measurements are independent.

As discussed in Section II, the statistics of the estimators are functions of the number of independent samples N. Thus it is important to obtain an accurate estimate of N from the measurements. In this work, we choose 50 samples out of the 100 samples by taking samples from every two stirrer rotation angles. In order to verify the independence of the selected 50 samples, we calculate the first order autocorrelation coefficient [4], [18] of different sets of samples (i.e., the 10 platform samples, the 5 stirrer samples and the total 50 samples) for all the nine measurements:

$$r(1) = \frac{\sum_{i=1}^{N} (s(i) - \bar{s})\,(s(i+1) - \bar{s})}{\sum_{i=1}^{N} (s(i) - \bar{s})^2}, \tag{29}$$

where s represents the measured S-parameters at each frequency, i.e., S_{11} for the one-antenna method and S_{21} for the three-antenna method. $\bar{s}$ represents the average of s.

Since the calculated $r(1)$ using the samples from nine measurements show good agreements, only one of the results is shown in Fig. 8. It can be seen from Figs. 8 (a) and (b) that $r(1)$ is below threshold $e^{-1}(\approx 0.37)$ over the whole bandwidth. Note that the threshold of e^{-1} is only suitable for a certain set of samples. For more accurate evaluation of independence, a modified threshold should be used [38], [39]. For the considered numbers of samples here (i.e., 5 and 10), the modified threshold is larger than e^{-1} [38], meaning that the 10 platform samples (5 stirrer samples) are independent with each other. To further verify the independence of the measured samples, both the autocorrelation function (ACF) method [38]–[40] and the degrees of freedom (DoF) method [36], [41] have been applied to the measured data. It is shown that the selected 50 samples are independent with each other. For the sake of conciseness, only $r(1)$ are shown here.

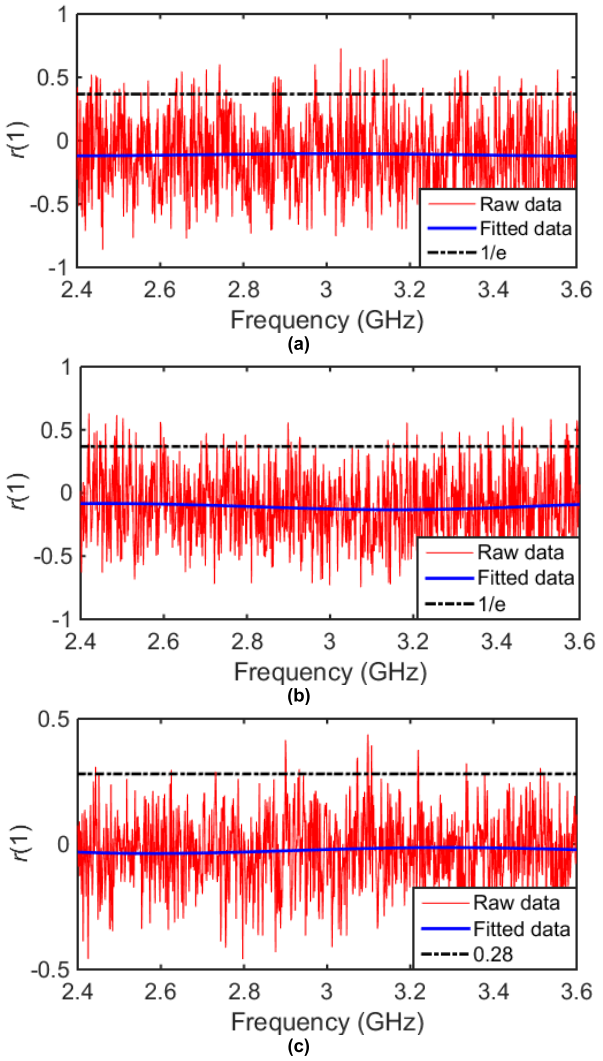

FIGURE 8. The first order autocorrelation coefficient $r(1)$ of different sets of samples: (a) 10 platform samples, (b) 5 stirrer samples, and (c) total 50 samples. Note that $1/e$ is the common threshold and 0.28 is the modified threshold [38] for 50 samples.

The RC decay time (τ_{RC}) is needed for the non-reference antenna methods. It can be obtained by processing S_{11}(for the one-antenna method) or S_{21} (for the three-antenna method) [11], [42]. Specifically, the power delay profile (PDP) can be

calculated as the inverse fast Fourier transform of S_{11} or S_{21} and τ_{RC} can be extracted from the PDP as

$$\tau_{RC} = -\frac{1}{slope\left\{\ln\left[PDP(t)\right]\right\}}, \tag{30}$$

where *slope* represents the slope operator of the linear part of its argument by curve fitting and ln denotes the natural logarithm. Specifically, τ_{RC} is calculated over the sub frequency range from 2.8 GHz to 3.2 GHz. Note that the S-parameters are sampled with a frequency step of 1 MHz at each stirrer position, thus we have total 400 frequency points to calculate τ_{RC}. Note that the coherence bandwidth of the used RC in this work is less than 1 MHz [17], so the samples in the sub frequency range can be regarded as uncorrelated.

For simplicity and without loss of generality, we measure the efficiency of Antenna 1 using the two non-reference antenna methods to further verify the derived statistics. The empirical statistics are directly calculated using the measurement results, while the analytical statistics are calculated using the derived estimators. It should be pointed that the efficiency of Antenna 1 is specifically measured in an anechoic chamber, which is used as the true antenna efficiency in the derived estimators [43], [44]. However, the measurement uncertainty of the total efficiency of Antenna 1 allows us to validate the statistical analysis presented in this paper.

Fig. 9 shows the empirical and analytical expectations and variances of estimator (1), the empirical MSEs of estimators (1) and (11) of the one-antenna method for $N = 50$. Since the estimator (11) is derived based on the estimator (1), the verifications of (1) and (11) are equivalent. Thus, we focus on the original estimator (1) for the sake of conciseness. In order to facilitate the comparison of different MSEs, we adopt the following dB-transformation [26], [35]

$$MSE_{dB} = 10\log_{10}\sqrt{\frac{1+MSE}{1-MSE}}. \tag{31}$$

As can be seen, the empirical expectations and variances are slightly larger than the analytical ones. It can be concluded from (10) that the mean of the measured antenna efficiency is proportional to the true antenna efficiency and the variance is proportional to the square of the true antenna efficiency. As discussed in [11], the measured antenna efficiency using the one-antenna method is higher than the true value because the true e_b is larger than two (i.e., $e_b > 2$) in our measurements. By assuming $e_b = 2$, the decrease of the actual value of e_b is transformed into a spurious increase of the antenna efficiency. This explains why the empirical expectations and variances are slightly larger than their analytical counterparts. The MSEs of estimators (1) and (11) are indistinguishable. This is in agreement with the analyses in Section III, i.e., the differences diminish for $N > 10$.

Fig. 10 shows the empirical and analytical expectations and variances of estimator (17), and the empirical MSEs of estimators (17) and (24) of the three-antenna method for $N = 50$. Similar to the one-antenna method, we focus on the original estimator (17) for the sake of conciseness. As can be seen, there are good agreement between the empirical and analytical expectation and variance. The MSEs of estimators (17) and (24) are indistinguishable. This is in agreement with the analyses in Section III.

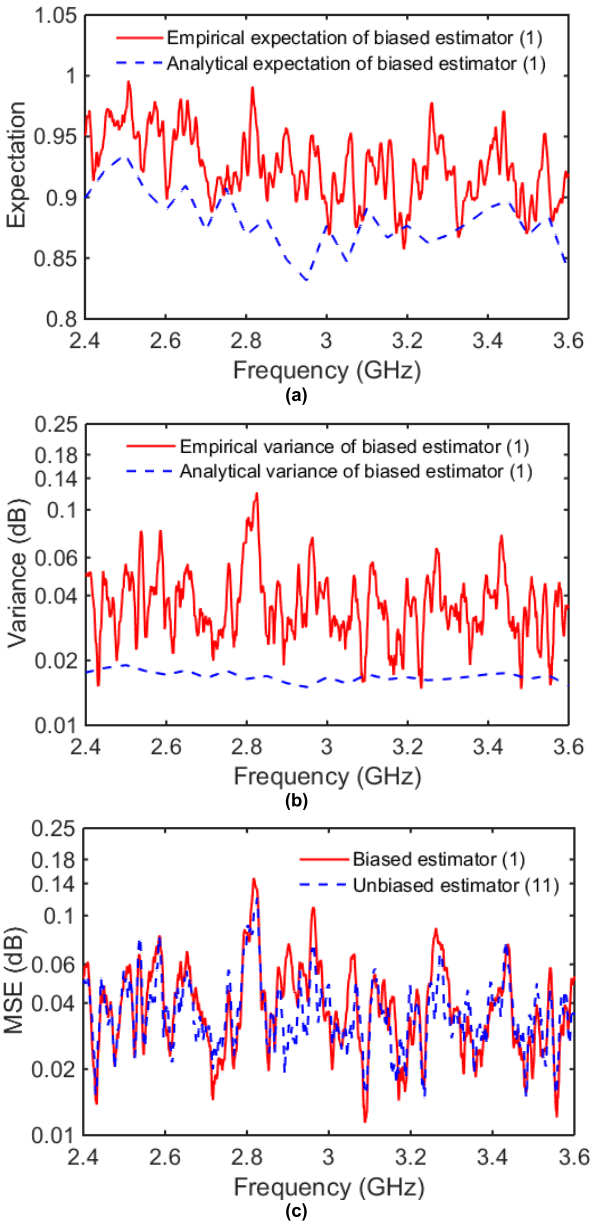

FIGURE 9. Measured statistics of the one-antenna method for $N = 50$: (a) empirical and analytical expectation, (b) empirical and analytical variance, and (c) empirical MSEs.

As mentioned in Section III, the PDF tends to concentrate around the true antenna efficiency as N grows larger. Thus increasing N can improve the measurement accuracy and reduce the fluctuations and biases. However, in order to verify the analytical statistics, we only take 50 samples and ensure that they are independent with each other. (Note that for an RC operating close to its lowest usable frequency [34],

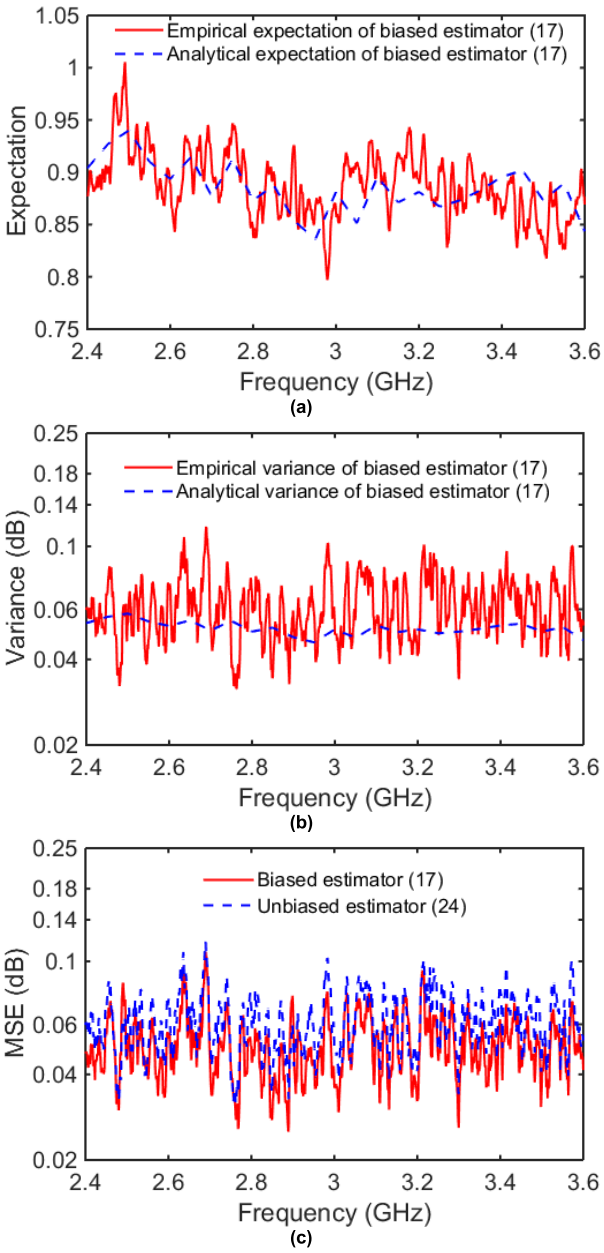

FIGURE 10. Measured statistics of the three-antenna method for $N = 50$: (a) empirical and analytical expectation, (b) empirical and analytical variance, and (c) empirical MSEs.

the maximum number of independent samples can be much smaller than 50.)

Comparing Fig. 9(a) and Fig. 10(a), it can be seen that the mean of the biased antenna efficiency measured using the one-antenna method is slightly higher than that obtained using the three-antenna method. This is in agreement with the empirical findings in [11], because the actual enhanced backscatter coefficient is slightly larger than two in the used RC. For further investigation of the effect of the enhanced backscatter coefficient, we calculate e_b of all the measurement configurations. Since the efficiency of Antenna 1 is

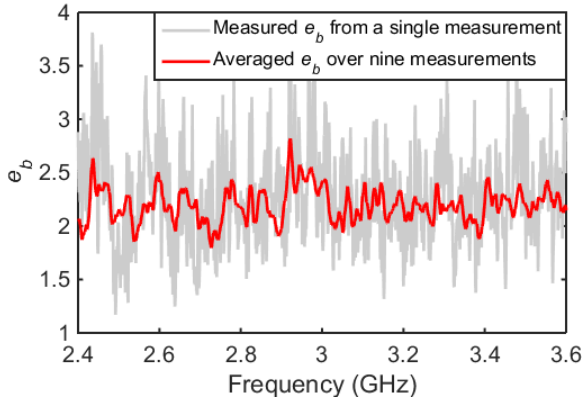

FIGURE 11. Measured e_b from a single measurement and averaged e_b over nine measurements using the combination of Antenna 1 and Antenna 2.

measured using the one- and three-antenna methods throughout this section, we select the combination of Antenna 1 and Antenna 2 to show e_b. Fig. 11 shows measured e_b from a single measurement and averaged e_b (using 5 MHz frequency stirring [45]) over nine measurements. It can be seen that the averaged e_b is larger than 2 and there is fluctuation of e_b. Overall, there are good agreement between the measured e_b from a single measurement and the averaged e_b over nine measurements, which indicates good stability of the measured e_b of the RC.

Finally, it should be noted that measurements of small reflection coefficients can be critical especially when long cables are used before the calibration planes of the VNA. In addition, the use of turn-table platform inevitably introduces some stress to the cable, which also affect the small reflection coefficient. Nevertheless, since the uncertainty contribution of small reflection coefficient is insignificant to the measured total antenna efficiency, its effect is omitted in the uncertainty analyses.

V. CONCLUSION

In this paper, we have derived the analytical distributions of the antenna efficiencies measured using two non-reference antenna methods in the RC. The statistics of the antenna efficiency estimators were obtained based on the derived distributions. Since estimators (1) and (17) were biased, the unbiased estimators (11) and (24) were proposed and compared with the biased ones. The analytically derived statistics of the estimators were verified by simulations and measurements. Good agreements were observed. The results showed that the unbiased estimator performed slightly better than the biased one for the three-antenna method when $N < 10$, while the biased estimator performed slightly better than the unbiased one for the one-antenna method. This indicates that the unbiased estimators can be used to improve the accuracy of the measurement only in specific cases. In addition, different non-reference antenna methods possess different biases for a specific N and different convergence rates as N

increases. Nevertheless, as the number of independent samples N grows larger (normally $N \leq N_{\text{meas}}$ with N_{meas} being the number of measured samples), the difference between the unbiased and biased estimators diminishes. The analytical expressions of the distributions and statistics derived in this work could enable more rigorous uncertainty analyses of the measured antenna efficiencies using the non-reference antenna methods.

APPENDIX

A. DERIVATION OF THE STATISTICS OF THE ONE-ANTENNA METHOD

Based on (8), the derivations of the first and second moments are given as follows:

$$\begin{aligned} E(t) &= \int tf(t)dt = \frac{2N^N}{\Gamma(N)}\int t^{2N}e^{-Nt^2}dt \\ &= \frac{2N^N}{\Gamma(N)}\frac{2N-1}{2N}\int t^{2N-2}e^{-Nt^2}dt \\ &= \frac{2N^N}{\Gamma(N)}\frac{(2N-1)(2N-3)}{(2N)^2}\int t^{2N-4}e^{-Nt^2}dt \\ &= \frac{2N^N}{\Gamma(N)}\frac{(2N-1)!!}{(2N)^N}\int e^{-Nt^2}dt \\ &= \frac{\Gamma(2N+1)}{\Gamma(N+1)^2}\frac{\sqrt{\pi N}}{2^{2N}}, \end{aligned} \tag{32}$$

$$\begin{aligned} E(t^2) &= \int t^2 f(t)dt = \frac{2N^N}{\Gamma(N)}\int t^{2N+1}e^{-Nt^2}dt \\ &= \frac{2N^N}{\Gamma(N)}\frac{2N}{2N}\int t^{2N-1}e^{-Nt^2}dt \\ &= \frac{2N^N}{\Gamma(N)}\frac{(2N)(2N-2)}{(2N)^2}\int t^{2N-3}e^{-Nt^2}dt \\ &= \frac{2N^N}{\Gamma(N)}\frac{2^N N!}{(2N)^N}\int te^{-Nt^2}dt = 1, \end{aligned} \tag{33}$$

where $2\int_0^{+\infty} e^{-Nx^2}dx = \sqrt{\pi/N}$ is known as the Gaussian integral.

Once $E(t)$ and $E(t^2)$ are obtained, the variance can be calculated using $D(t) = E(t^2) - [E(t)]^2$. Furthermore, we can obtain $E\left(\hat{e}_1\right) = e_1 E(t)$ and $D\left(\hat{e}_1\right) = e_1^2 D(t)$ [i.e., (10)]. Note that $E(\hat{e}_1)$ and $D\left(\hat{e}_1\right)$ can also be derived from (9) directly.

The CRLB for the variance of the unbiased estimator of the distribution parameter is given in [31]

$$CRLB(a) = \frac{1}{NI(a)}, \tag{34}$$

where N is the sample number, a is the distribution parameter being estimated, $I(a)$ is the Fisher information and can be calculated using

$$I(a) = -E\left[\frac{\partial^2 \ln(f(X;a))}{\partial a}\right] = E\left[\left(\frac{\partial \ln(f(X;a))}{\partial a}\right)^2\right], \tag{35}$$

where ∂ is the partial derivative operator, $f(X;a)$ is the PDF of random variable X and depends on the distribution parameter a.

Based on (9), the Fisher information of e_1 can be calculated as

$$I(e_1) = -E\left[\frac{\partial^2 \ln(f(g;e_1))}{\partial e_1^2}\right] = \frac{6N}{e_1^4}E(g^2) - \frac{2N}{e_1^2} = \frac{4N}{e_1^2}. \tag{36}$$

Thus, the CRLB can be obtained as

$$CRLB(e_1) = \frac{1}{NI(e_1)} = \frac{e_1^2}{4N^2}. \tag{37}$$

B. DERIVATION OF THE STATISTICS OF THE THREE-ANTENNA METHOD

The derivation of the PDF of the three-antenna method is given as follow:

$$\begin{aligned} f(w) &= \int f_Z(wv)f_V(v)\,|v|\,dv \\ &= \frac{8N^{3N}A^{4N}}{\Gamma(N)^3}w^{2N-1}\int v^{4N-1}e^{-A^2Nv^2}K_0(2ANwv)dv \\ &= \frac{2N^{N-1/2}\Gamma(2N)^2}{\Gamma(N)^3}w^{2N-2}e^{Nw^2/2}W_{(1/2-2N,0)}(Nw^2) \\ &= \frac{2N^N\Gamma(2N)^2}{\Gamma(N)^3}w^{2N-1}U(2N,1,Nw^2) \\ &= \frac{2\Gamma(2N)^2}{\Gamma(N)^3N^Nw^{2N+1}}{}_2F_0(2N,2N;;-\frac{1}{Nw^2}), \end{aligned} \tag{38}$$

where $W_{\lambda,\mu}(x)$ represents the Whittaker function of the second kind [30] and $U(a,b,z)$ represents the confluent hypergeometric function of the second kind [30].

The derivations of the first and second moments are given as follows:

$$\begin{aligned} E(w) &= \int wf(w)du \\ &\overset{x=Nw^2}{=} \frac{\Gamma(2N)^2}{\sqrt{N}\Gamma(N)^3}\int x^{N-1}e^{x/2}W_{(1/2-2N,0)}(x)dx \\ &= \frac{1}{\sqrt{N}\Gamma(N)^3}\int x^{N-1}G_{1,2}^{2,1}(x\,\Big|^{3/2-2N}_{1/2,1/2})dx \\ &= \frac{\Gamma(N+\frac{1}{2})^2\Gamma(N-\frac{1}{2})}{\sqrt{N}\Gamma(N)^3}, \end{aligned} \tag{39}$$

$$\begin{aligned} E\left(w^2\right) &= \int w^2 f(w)du \\ &\overset{x=Nw^2}{=} \frac{\Gamma(2N)^2}{N\Gamma(N)^3}\int x^{N-1/2}e^{x/2}W_{(1/2-2N,0)}(x)dx \\ &= \frac{1}{N\Gamma(N)^3}\int x^{N-1/2}G_{1,2}^{2,1}(x\,\Big|^{3/2-2N}_{1/2,1/2})dx \\ &= \frac{\Gamma(N+1)^2\Gamma(N-1)}{N\Gamma(N)^3}, \end{aligned} \tag{40}$$

where $G_{p,q}^{m,n}\left(x\,\Big|^{a_1,\ldots a_n,a_{n+1},\ldots a_p}_{b_1,\ldots b_m,b_{m+1},\ldots b_q}\right)$ represents the Meijer's G-function [46].

Similar to the one-antenna method, the variance can be calculated using $D(w) = E(w^2) - [E(w)]^2$. Furthermore, we can obtain $E\left(\hat{e}_1\right) = e_1 E\left(w\right)$ and $D\left(\hat{e}_1\right) = e_1^2 D\left(w\right)$ [i.e., (23)].

The Fisher information of e_1 can be calculated from (22) as

$$\begin{aligned} I(e_1) &= E\left[\frac{\partial \ln(f(r;e_1))}{\partial e_1}\right]^2 \\ &= E\left[\left(-\frac{2N}{e_1} + \frac{\partial \ln(U(2N,1,Nr^2/e_1^2))}{\partial e_1}\right)^2\right] \\ &= E\left[\left(-\frac{2N}{e_1} + \frac{4N^2r^2}{e_1^3}\frac{U(2N+1,2,Nr^2/e_1^2)}{U(2N,1,Nr^2/e_1^2)}\right)^2\right]. \end{aligned} \tag{41}$$

Thus, the CRLB can be obtained as

$$CRLB(e_1) = \frac{1}{NI(e_1)}. \tag{42}$$

REFERENCES

[1] D. A. Hill, *Electromagnetic Fields in Cavities: Deterministic and Statistical Theories*. Piscataway, NJ, USA, USA: Wiley, 2009.

[2] V. Rajamani, C. F. Bunting, and J. C. West, "Stirred-mode operation of reverberation chambers for EMC testing," *IEEE Trans. Instrum. Meas.*, vol. 61, no. 10, pp. 2759–2764, Oct. 2012, doi: 10.1109/TIM.2012.2196398.

[3] H. Zhao, "MLFMM-accelerated integral-equation modeling of reverberation chambers [open problems in CEM]," *IEEE Antennas Propag. Mag.*, vol. 55, no. 5, pp. 299–308, Oct. 2013, doi: 10.1109/MAP.2013.6735541.

[4] *Electromagnetic Compatibility (EMC)—Part 4-21: Testing and Measurement Techniques—Reverberation Chamber Test Methods*, Standard IEC 61000-4-21, International Electrotechnical Commission, 2011.

[5] X. Chen, J. Tang, T. Li, S. Zhu, Y. Ren, Z. Zhang, and A. Zhang, "Reverberation chambers for Over-the-Air tests: An overview of two decades of research," *IEEE Access*, vol. 6, pp. 49129–49143, 2018, doi: 10.1109/ACCESS.2018.2867228.

[6] D. Micheli, M. Barazzetta, C. Carlini, R. Diamanti, V. M. Primiani, and F. Moglie, "Testing of the carrier aggregation mode for a live LTE base station in reverberation chamber," *IEEE Trans. Veh. Technol.*, vol. 66, no. 4, pp. 3024–3033, Apr. 2017, doi: 10.1109/TVT.2016.2587662.

[7] M. Barazzetta, D. Micheli, L. Bastianelli, R. Diamanti, M. Totta, P. Obino, R. Lattanzi, F. Moglie, and V. M. Primiani, "A comparison between different reception diversity schemes of a 4G-LTE base station in reverberation chamber: A deployment in a live cellular network," *IEEE Trans. Electromagn. Compat.*, vol. 59, no. 6, pp. 2029–2037, Dec. 2017, doi: 10.1109/TEMC.2017.2657122.

[8] W. Fan, P. Kyosti, M. Rumney, X. Chen, and G. F. Pedersen, "Over-the-Air radiated testing of millimeter-wave beam-steerable devices in a cost-effective measurement setup," *IEEE Commun. Mag.*, vol. 56, no. 7, pp. 64–71, Jul. 2018, doi: 10.1109/MCOM.2018.1701006.

[9] *'Test Plan forWireless Large-Form-Factor Device Over-the-Air Performance' Version Number: 1.2*, CTIA Certification, Washington, DC, USA:, 2017.

[10] H. G. Krauthäuser and M. Herbrig, "Yet another antenna efficiency measurement method in reverberation chambers," in *Proc. IEEE Int. Symp. Electromagn. Compat., Fort Lauderdale*, Jul. 2010, pp. 536–540, doi: 10.1109/ISEMC.2010.5711333.

[11] C. L. Holloway, H. A. Shah, R. J. Pirkl, W. F. Young, D. A. Hill, and J. Ladbury, "Reverberation chamber techniques for determining the radiation and total efficiency of antennas," *IEEE Trans. Antennas Propag.*, vol. 60, no. 4, pp. 1758–1770, Apr. 2012, doi: 10.1109/TAP.2012.2186263.

[12] A. Khaleghi, "Time-domain measurement of antenna efficiency in reverberation chamber," *IEEE Trans. Antennas Propag.*, vol. 57, no. 3, pp. 817–821, Mar. 2009, doi: 10.1109/TAP.2009.2013445.

[13] G. Le Fur, P. Besnier, and A. Sharaiha, "Time reversal efficiency measurement in reverberation chamber," *IEEE Trans. Antennas Propag.*, vol. 60, no. 6, pp. 2921–2928, Jun. 2012, doi: 10.1109/TAP.2012.2194631.

[14] A. Gifuni, I. D. Flintoft, S. J. Bale, G. C. R. Melia, and A. C. Marvin, "A theory of alternative methods for measurements of absorption cross section and antenna radiation efficiency using nested and contiguous reverberation chambers," *IEEE Trans. Electromagn. Compat.*, vol. 58, no. 3, pp. 678–685, Jun. 2016, doi: 10.1109/TEMC.2016.2548939.

[15] D. Senic, D. F. Williams, K. A. Remley, C.-M. Wang, C. L. Holloway, Z. Yang, and K. F. Warnick, "Improved antenna efficiency measurement uncertainty in a reverberation chamber at millimeter-wave frequencies," *IEEE Trans. Antennas Propag.*, vol. 65, no. 8, pp. 4209–4219, Aug. 2017, doi: 10.1109/TAP.2017.2708084.

[16] P. Besnier, J. Sol, A. Presse, C. Lemoine, and A.-C. Tarot, "Antenna efficiency measurement from quality factor estimation in reverberation chamber," in *Proc. 46th Eur. Microw. Conf. (EuMC)*, Oct. 2016, pp. 715–718, doi: 10.1109/EuMC.2016.7824443.

[17] P.-S. Kildal, C. Carlsson, and J. Yang, "Measurement of free-space impedances of small antennas in reverberation chambers," *Microw. Opt. Technol. Lett.*, vol. 32, no. 2, pp. 112–115, Jan. 2002, doi: 10.1002/mop.10105.

[18] G. Andrieu, N. Ticaud, F. Lescoat, and L. Trougnou, "Fast and accurate assessment of the 'well stirred condition' of a reverberation chamber from S_{11} measurements," *IEEE Trans. Electromagn. Compat.*, vol. 61, no. 4, pp. 974–982, Aug. 2019, doi: 10.1109/TEMC.2018.2847727.

[19] M. A. Garcia-Fernandez, D. Carsenat, and C. Decroze, "Antenna radiation pattern measurements in reverberation chamber using plane wave decomposition," *IEEE Trans. Antennas Propag.*, vol. 61, no. 10, pp. 5000–5007, Oct. 2013, doi: 10.1109/TAP.2013.2271631.

[20] V. Fiumara, A. Fusco, V. Matta, and I. M. Pinto, "Free-space antenna field/pattern retrieval in reverberation environments," *IEEE Antennas Wireless Propag. Lett.*, vol. 4, pp. 329–332, 2005, doi: 10.1109/LAWP.2005.855633.

[21] C. Lemoine, E. Amador, P. Besnier, J.-M. Floc'h, and A. Laisne, "Antenna directivity measurement in reverberation chamber from rician K-factor estimation," *IEEE Trans. Antennas Propag.*, vol. 61, no. 10, pp. 5307–5310, Oct. 2013, doi: 10.1109/TAP.2013.2272691.

[22] A. Cozza and A. el-Bassir Abou el-Aileh, "Accurate radiation-pattern measurements in a time-reversal electromagnetic chamber," *IEEE Antennas Propag. Mag.*, vol. 52, no. 2, pp. 186–193, Apr. 2010, doi: 10.1109/MAP.2010.5525625.

[23] Q. Xu, Y. Huang, L. Xing, C. Song, Z. Tian, S. S. Alja'afreh, and M. Stanley, "3-D antenna radiation pattern reconstruction in a reverberation chamber using spherical wave decomposition," *IEEE Trans. Antennas Propag.*, vol. 65, no. 4, pp. 1728–1739, Apr. 2017, doi: 10.1109/TAP.2016.2633901.

[24] X. Chen, P.-S. Kildal, J. Carlsson, and J. Yang, "MRC diversity and MIMO capacity evaluations of multi-port antennas using reverberation chamber and anechoic chamber," *IEEE Trans. Antennas Propag.*, vol. 61, no. 2, pp. 917–926, Feb. 2013, doi: 10.1109/TAP.2012.2223442.

[25] J. F. Valenzuela-Valdes, M. A. Garcia-Fernandez, A. M. Martinez-Gonzalez, and D. A. Sanchez-Hernandez, "The influence of efficiency on receive diversity and MIMO capacity for Rayleigh-fading channels," *IEEE Trans. Antennas Propag.*, vol. 56, no. 5, pp. 1444–1450, May 2008, doi: 10.1109/TAP.2008.922208.

[26] X. Chen, "On statistics of the measured antenna efficiency in a reverberation chamber," *IEEE Trans. Antennas Propag.*, vol. 61, no. 11, pp. 5417–5424, Nov. 2013, doi: 10.1109/TAP.2013.2276920.

[27] G. Andrieu and N. Ticaud, "Performance comparison and critical examination of the most popular stirring techniques in reverberation chambers using the 'well-stirred' condition method," *IEEE Trans. Electromagn. Compat.*, vol. 62, no. 1, pp. 3–15, Feb. 2020, doi: 10.1109/TEMC.2019.2926331.

[28] J. Ladbury and D. A. Hill, "Enhanced backscatter in a reverberation chamber: Inside every complex problem is a simple solution struggling to get out," in *Proc. IEEE Int. Symp. Electromagn. Compat.*, Honolulu, HI, USA, Jul. 2007, pp. 1–5, doi: 10.1109/ISEMC.2007.201.

[29] G. Grimmett and D. Stirzaker, *Probability and Random Processes*, 3rd ed. New York, NY, USA: Oxford Univ. Press, 2001.

[30] M. Abramowitz and I. A. Stegun, *Handbook of Mathematical Functions with Formulas, Graphs, and Mathematical Tables*. New York, NY, USA: Dover, 1972.

[31] H. Cramér, *Mathematical Methods of Statistics*. Princeton, NJ, USA: Princeton Univ. Press, 1999.

[32] V. Fiumara, A. Fusco, G. Iadarola, V. Matta, and I. M. Pinto, "Free-space antenna pattern retrieval in nonideal reverberation chambers," *IEEE Trans. Electromagn. Compat.*, vol. 58, no. 3, pp. 673–677, Jun. 2016, doi: 10.1109/TEMC.2016.2539351.
[33] Q. Xu, L. Xing, Z. Tian, Y. Zhao, X. Chen, L. Shi, and Y. Huang, "Statistical distribution of the enhanced backscatter coefficient in reverberation chamber," *IEEE Trans. Antennas Propag.*, vol. 66, no. 4, pp. 2161–2164, Apr. 2018, doi: 10.1109/TAP.2018.2800782.
[34] V. Mariani Primiani and F. Moglie, "Numerical simulation of reverberation chamber parameters affecting the received power statistics," *IEEE Trans. Electromagn. Compat.*, vol. 54, no. 3, pp. 522–532, Jun. 2012, doi: 10.1109/TEMC.2011.2167337.
[35] P.-S. Kildal, X. Chen, C. Orlenius, M. Franzen, and C. S. L. Patane, "Characterization of reverberation chambers for OTA measurements of wireless devices: Physical formulations of channel matrix and new uncertainty formula," *IEEE Trans. Antennas Propag.*, vol. 60, no. 8, pp. 3875–3891, Aug. 2012, doi: 10.1109/TAP.2012.2201125.
[36] X. Chen, "Experimental investigation of the number of independent samples and the measurement uncertainty in a reverberation chamber," *IEEE Trans. Electromagn. Compat.*, vol. 55, no. 5, pp. 816–824, Oct. 2013, doi: 10.1109/TEMC.2013.2242473.
[37] K. A. Remley, J. Dortmans, C. Weldon, R. D. Horansky, T. B. Meurs, C.-M. Wang, D. F. Williams, C. L. Holloway, and P. F. Wilson, "Configuring and verifying reverberation chambers for testing cellular wireless devices," *IEEE Trans. Electromagn. Compat.*, vol. 58, no. 3, pp. 661–672, Jun. 2016, doi: 10.1109/TEMC.2016.2549031.
[38] N. Wellander, O. Lundn, and M. Bckstrm, "Experimental investigation and mathematical modeling of design parameters for efficient stirrers in mode-stirred reverberation chambers," *IEEE Trans. Electromagn. Compat.*, vol. 49, no. 1, pp. 94–103, Feb. 2007, doi: 10.1109/TEMC.2006.888166.
[39] S. Pfennig, "A general method for determining the independent stirrer positions in reverberation chambers: Adjusting the correlation threshold," *IEEE Trans. Electromagn. Compat.*, vol. 58, no. 4, pp. 1252–1258, Aug. 2016, doi: 10.1109/TEMC.2016.2567541.
[40] G. Gradoni, V. Mariani Primiani, and F. Moglie, "Reverberation chamber as a multivariate process: FDTD evaluation of correlation matrix and independent positions," *Prog. Electromagn. Res.*, vol. 133, pp. 217–234, 2013, doi: 10.2528/PIER12091807.
[41] R. J. Pirkl, K. A. Remley, and C. S. L. Patane, "Reverberation chamber measurement correlation," *IEEE Trans. Electromagn. Compat.*, vol. 54, no. 3, pp. 533–544, Jun. 2012, doi: 10.1109/TEMC.2011.2166964.
[42] C. L. Holloway, H. A. Shah, R. J. Pirkl, K. A. Remley, D. A. Hill, and J. Ladbury, "Early time behavior in reverberation chambers and its effect on the relationships between coherence bandwidth, chamber decay time, RMS delay spread, and the chamber buildup time," *IEEE Trans. Electromagn. Compat.*, vol. 54, no. 4, pp. 714–725, Aug. 2012, doi: 10.1109/TEMC.2012.2188896.
[43] C.A. Balanis, *Antenna Theory: Analysis and Design*. Hoboken, NJ, USA: Wiley, 2005.
[44] Y. Huang, "Radiation efficiency measurements of small antennas," in *Handbook of Antenna Technologies*, Z. Chen, Ed. Singapore: Springer, 2015.
[45] J. C. West and C. F. Bunting, "Effects of frequency stirring on reverberation chamber testing: An analysis as a radiation problem," *IEEE Trans. Electromagn. Compat.*, vol. 61, no. 4, pp. 1345–1352, Aug. 2019, doi: 10.1109/TEMC.2019.2919913.
[46] A. M. Mathai, *A Handbook of Generalized Special Functions for Statistical and Physical Sciences*. New York, NY, USA: Oxford Univ. Press, 1993.

WEI XUE (Student Member, IEEE) received the B.S. and M.S. degrees from Xi'an Jiaotong University, Xi'an, China, in 2011 and 2014, respectively, where he is currently pursuing the Ph.D. degree in electronics science and technology. From 2014 to 2018, he was an Avionic Engineer with the Aeronautic Computing Technology Institute, Xi'an. His current research interests include reverberation chamber, over-the-air (OTA) testing, and statistical electromagnetic.

XIAOMING CHEN (Senior Member, IEEE) received the B.Sc. degree in electrical engineering from Northwestern Polytechnical University, Xi'an, China, in 2006, and the M.Sc. and Ph.D. degrees in electrical engineering from the Chalmers University of Technology, Gothenburg, Sweden, in 2007 and 2012, respectively. From 2013 to 2014, he was a Postdoctoral Researcher with the Chalmers University of Technology. From 2014 to 2017, he was with Qamcom Research and Technology AB, Gothenburg, where he was involved in the EU H2020 5GPPP mmMAGIC Project (on 5G millimeter-wave wireless access techniques). Since 2017, he has been a Professor with Xi'an Jiaotong University, Xi'an. His research interests include 5G multi-antenna techniques, over-the-air (OTA) testing, and reverberation chambers. He has coauthored one book, two book chapters, and more than 80 journal articles on these topics. He received the International Union of Radio Science (URSI) Young Scientist Awards, in 2017 and 2018, and the IEEE Outstanding AE Awards, in 2018 and 2019. He serves as an Associate Editor (AE) for the journal of the IEEE Antennas and Wireless Propagation Letters (AWPL). He was also a Guest Editor of a Special Cluster on 5G/6G Enabling Antenna Systems and Associated Testing Technologies in AWPL and a Special Issue on Metrology for 5G Technologies in the journal of *IET Microwaves, Antennas and Propagation*.

MING ZHANG (Member, IEEE) received the B.S. and M.S. degrees in information and communications engineering and the Ph.D. degree in electronic science and technology from Xi'an Jiaotong University, Xi'an, China, in 2008, 2011, and 2017, respectively. From 2011 to 2014, he was with Huawei Technologies Company Ltd. From 2018 to 2019, he was a Postdoctoral Researcher with Xi'an Jiaotong University, where he is currently an Associate Professor with the School of Information and Communications Engineering. His research interests include array signal processing and linear system analysis, with applications to radar, wireless communications, and satellite navigations.

LUYU ZHAO (Senior Member, IEEE) was born in Xi'an, China, in 1984. He received the B.Eng. degree from Xidian University, Xi'an, in 2007, and the Ph.D. degree from The Chinese University of Hong Kong, Shatin, Hong Kong, in 2014. From 2007 to 2009, he was with the Key Laboratory of Antennas and Microwave Technology, Xidian University, as a Research Assistant, where he was involved with software and hardware implementation of RF identification (RFID) technologies. From 2014 to 2015, he was a Postdoctoral Fellow with The Chinese University of Hong Kong. From October 2015 to October 2016, he was with Wyzdom Wireless Company Ltd., where he was a Co-Founder and the CTO. He has been an Associate Professor with the National Key Laboratory of Antennas and Microwave Technology, Xidian University, since 2016. His current research interests include design and application of multiple antenna systems for next-generation mobile communication systems, innovative passive RF and microwave components and systems, millimeter wave and terahertz antenna array, meta-material based or inspired antenna arrays. He was a recipient of the Best Student Paper Award of 2013 IEEE 14th HK AP/MTT Postgraduate Conference and the Honorable Mention Award of 2017 Asia-Pacific Conference on Antenna and Propagation. He has been serving as an Associate Editor for the journal IEEE Access.

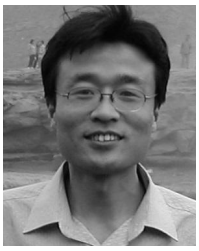

ANXUE ZHANG (Member, IEEE) received the B.S. degree in electrical and electronics engineering from Henan Normal University, in 1996, and the M.S. and Ph.D. degrees in electromagnetic and microwave engineering from Xi'an Jiaotong University, Xi'an, China, in 1999 and 2003, respectively. He is currently a Professor with Xi'an Jiaotong University. His research interests include antenna and electromagnetic wave propagation, RF and microwave circuit design, and metamaterials, with applications to radar and wireless communications.

YI HUANG (Senior Member, IEEE) received the B.Sc. degree in physics from Wuhan University, China, in 1984, the M.Sc. (Eng.) degree in microwave engineering from NRIET, Nanjing, China, in 1987, and the D.Phil. degree in communications from the University of Oxford, U.K., in 1994. He has been conducting research in the areas of wireless communications, applied electromagnetics, radar and antennas, since 1987. His experience includes three years spent with NRIET, as a Radar Engineer and various periods with the Universities of Birmingham, Oxford, and Essex, U.K., as a Member of Research Staff. He has worked as a Research Fellow with British Telecom Labs, in 1994, and then joined the Department of Electrical Engineering and Electronics, University of Liverpool, U.K., as a Faculty, in 1995, where he is currently a Full Professor in wireless engineering, the Head of the High Frequency Engineering Group, and the Deputy Head of the Department. He has published over 350 refereed papers in leading international journals and conference proceedings. He has received many research grants from research councils, government agencies, charity, EU, and industry. He was a recipient of eight awards such as the BAE Systems Chairman's Award 2017, the IET Innovation Award 2018, and the Best Paper Awards. He has served on a number of national and international technical committees and been an Editor, an Associate Editor, or a Guest Editor for five international journals.